MAT - 010

Proceeding Seminar Nasional Tahunan Teknik Mesin XI (SNTTM XI) & Thermofluid IV
Universitas Gadjah Mada (UGM), Yogyakarta, 16-17 Oktober 2012

Isothermal oxidation behavior of aluminized AISI 1020 steel at the temperature of 700 °C

Mohammad Badaruddin[1*], Suharno[2], Hanif Ari Wijaya[1]

[1])Mechanical Engineering Department, Engineering Faculty, Lampung University
[2])Engineering Geophysics Department, Engineering Faculty, Lampung University
Jalan Prof. S. Brojonegoro No.1 Bandar Lampung, 35145, Indonesia
*Corresponding author: mbruddin@unila.ac.id

Abstract

The AISI 1020 steel was coated by dipping into the molten Al bath at 700 °C for 16s. The coating layer formed on the steel substrate is consisting of Al with a little Fe, $FeAl_3$ and Fe_2Al_5 layers. The morphologies of the $FeAl_3$ and Fe_2Al_5 layers are platelet and columnar structures, respectively. The oxidation test was carried out isothermally at 700 °C for a various time of 1–49 h in static air. The oxidation behaviors of both of the bare steel and the aluminized steel were studied by the oxidation kinetics, surface morphologies and phase transformation after oxidation testing. The oxidation products were characterized using Optical Microscope (OM), Scanning Electron Microscopy with Electron Dispersive Spectroscopy (SEM/EDS) and X-ray diffraction analysis. The rate constant (k_p) of the aluminized steel is two order lower than the bare steel. The formations of intermetallic phases on the steel substrate for a shorter time are dominated by the interdiffusion between the inward diffusion of Al-atoms into the steel substrate and outward diffusion of Fe-atoms. The constituent phases in the aluminide layer compose of $FeAl_2$, Fe_2Al_5 and $FeAl$. The formation of FeAl phase is controlled by the inward diffusion of Fe-atoms into the Fe_2Al_5 phase. The improvement of the oxidation resistance of the aluminized steel subjected to severe oxidation is due to the formation of protective Al_2O_3 scale.

Keywords: *aluminized AISI 1020 steel, oxidation kinetics, intermetallic phase, Al_2O_3*

1. Introduction

Low carbon steel, AISI 1020, is relatively low price and its corrosion resistance at high temperatures can be increased by hot-dip aluminizing coating method. This steel can be manufactured for engineering components such as pressure vessels, boiler, gas or oil pipelines. Hot-dip aluminum coating method was chosen because this method is cheap and able to be mass produced for a large component, complex and asymmetric shapes.

Corrosion is as result of chemical reactions between corrosive gases and metal (Qiao & Yan 1998). Even a leak of gas pipeline often occurs without an early identification because of the high concentration of sulfur and chloride gases in the enviromental surrounding (Kalidova et al 2005 & Erlindo et al 2010). Due to a high concentration of corrosive gases, such as in Ulubelu geothermal production field of Lampung Province, thus design process of pipeline for steam production in geothermal wells should always pay specially attention againts corrosion resistance and strength of the materials to prevent catastrophic failure during operation when the line is filled with oil or steam (Ghosh 2007). Application of protective coating, such as hot-dip Al coating can suitably be used on the pipe to replace the use of stainless steel or titanium (Cédric 2005). So the production and maintenance cost can be minimazed.

The present work focuses on the investigation of high-temperature oxidation of low carbon steel with aluminizing coating at 700 °C. This temperature represents the high limit of temperature that may be experienced by a steel pipe in high temperature condition. Reaction rates, morphology of reaction products, and composition changes occurring in the aluminized steel, are examined to provide an insight into the oxidation mechanisms.

2. Experimental Procedure

The substrates were cut into coupons with the sizes of 20 mm ×10 mm ×1 mm from the commercial AISI 1020 steel with composition (wt.%); 0.2C–0.5Mn–0.04P–0.05S and Fe–balance. Before hot dip aluminizing all specimens were cleaned by 5% NaOH and 10% H_3PO_4, and then coated by uniform Al welding flux. The Al ingot with 99.9 wt.% was melted in an alumina crucible and maintained at 700 °C. The specimens, fixed by a hook made of stainless steel wire. The up/down speed of the specimen elevator was 15 cm/min. After 16 s of immersion, they were pulled out and air-cooled to room temperature. The oxide flux deposited on the

surface of the aluminized specimens was then cleaned using a nitric acid, phosphoric acid, and water solution (1:1:1 v/v) at room temperature.

In order to investigate the oxidation behavior of the bare and the aluminized steel, all specimens were exposed in a box furnace at 700 °C for various duration of time 49 h. After a given isothermal oxidation time, the specimens were taken out and cooled in air at room temperature. Each weight gain data point for the oxidation kinetics was obtained from a different specimen. Only aluminized specimens were characterized as following; structures of scale and phases formation were identified by X-ray diffraction (XRD) using monochromatic Cu-Kα, the cross-sectional micrograph was taken by optical microscope (OM), the surface morphology and cross-sections of the specimens and chemical composition (at.%) were examined using scanning electron microscopy (SEM) with secondary electron image (SEI) signals and energy dispersive spectroscopy (EDS).

3. Results and Discussion

3.1 Oxidation kinetics

The aluminized and bare steel were isothermally oxidized at 700 °C for 49 h in static air. The oxidation kinetics curve is shown in Figure 1. Figure 1a shows changes in weight gain per unit surface area versus time, revealing that the kinetics curves approximately obeyed the parabolic rate law. In addition, it can be seen that the weight gain of specimens increases with increasing temperature. At the oxidation time approximately 8 h, the oxidation rate runs rapidly. In this stage, the oxidation rate is controlled by the oxygen/metal reaction. Whereas, after oxidation time of 8 h, the oxidation rate of coated specimen increases gradually, indicating that the Al-rich oxide scales formed on the surfaces can act as a diffusion barrier. However, the aluminized steel shows a lower than bare steel in weight gain. The bare steel shows a high oxidation rate in increasing of weight gains, indicating that the AISI 1020 steel cannot withstand oxidation attack at 700 °C for 49 h in air environment. The aluminized steel shows much improved oxidation resistance. The aluminide coating exhibits excellent high temperature oxidation protection due to the formation of a protective alumina scale (Al_2O_3). After being oxidized for 49 h, the weight gain of the coated specimen is approximately 0.388 mg/cm^2, only about 1/38 of the uncoated specimen (14.69 mg/cm^2). The kinetics rate, k_p, was calculated from Figure 1b, using the equation of $\Delta W = k_p t^{1/2}$, where ΔW is the weight gain per unit are and t is the oxidation time. The kinetics rates of the bare and the aluminized steel, are approximately 8.456×10^{-10} and 1.073×10^{-12} g^2 cm^{-4}

s^{-1}, respectively. The k_p value of the aluminized steel in this study is almost similar to the previous work (Badaruddin 2011). The formation of protective Al_2O_3 layer takes place to control the diffusion reaction of outward Al-cations and inward O-anions through the oxide. Therefore, the kinetics rate is decreased very significantly.
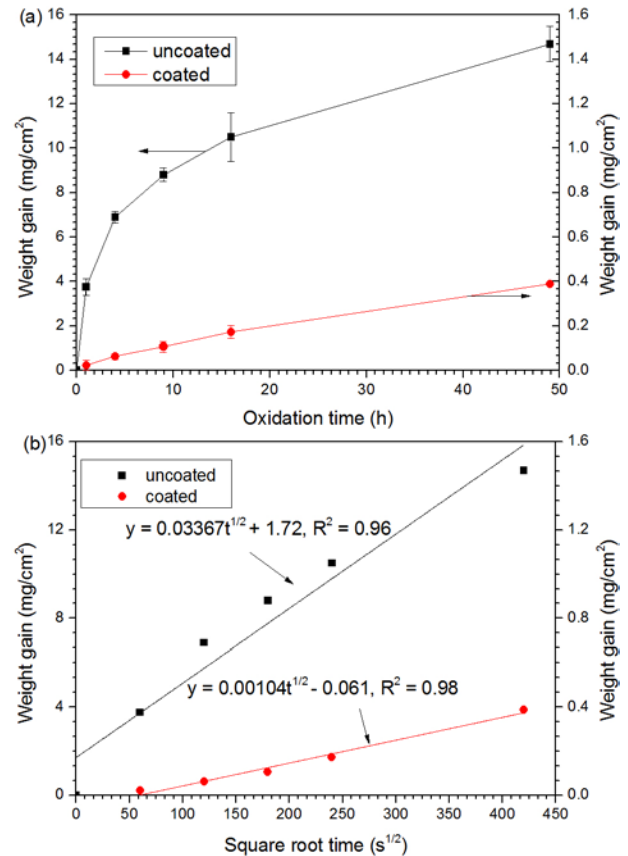

Figure 1 (a) Plot of linear oxidation kinetics and (b) parabolic oxidation kinetics

3.2. Microstructures and XRD examinations

Figure 2 shows mainly two coating layers; one is Al-layer with poor Fe, and the others is intermetallic layer consisting of $FeAl_3$ and Fe_2Al_5 layer. The XRD pattern is shown in Figure 2 for the coated sample. This sample, after the hot-dipping step, was lightly centrifuged so as to remove as much aluminum from its surface as possible. The purpose was to be able to reach the intermetallic layer with minimal grinding. In these XRD patterns, the diffraction peaks from aluminum (FCC) and intermetallic compounds have been marked with suitable symbols.

It can also be observed that the phase of $FeAl_3$ formed between Al matrix and Fe_2Al_5 phase shows the exterior of the structure is platelet, while the morphology such as the tongue-like can be seen clearly on the phase of Fe_2Al_5. This morphology is generally found on the hot-dip aluminized steel with an approximately 99.9 wt% Al (pure Al). The uniform

thickness of Al layer and the intermetallic layer are approximately 10 μm in outermost and approximately 50 μm in innermost, respectively. The aluminide layer seems to be homogenous and good adherence to the steel substrate. No pores and crack can be seen, which is common in the Al-diffusion coating formed after hot-dipping process. The composition of $FeAl_3$ and Fe_2Al_5 are about 80.02Al−19.8Fe and 69.29Al−30.691Fe (at.%), respectively. Besides that, the tongue-like morphology is associated with vacancy defects owned by Fe_2Al_5 phase about 30% and therefore, Al can diffuse more rapidly into the steel substrate than the outward diffusion of Fe atom during immersion of steel into a molten Al bath. In addition, these vacancies provide easy diffusion paths in the c direction, contributing to the rapid growth of the Fe_2Al_5 phase (Cheng & Wang 2009). This phase growth is controlled by temperature, where the diffusion coefficient of Al atom is higher in solid Fe; 53×10^{-4} m^2s^{-1} at the temperature range of 520−650 °C, and the diffusion coefficient of the iron atom (Fe); 1.8×10^{-4} m^2s^{-1} at the temperature range of 830−1400 °C (Kamey 1996 & Neumann 1999).
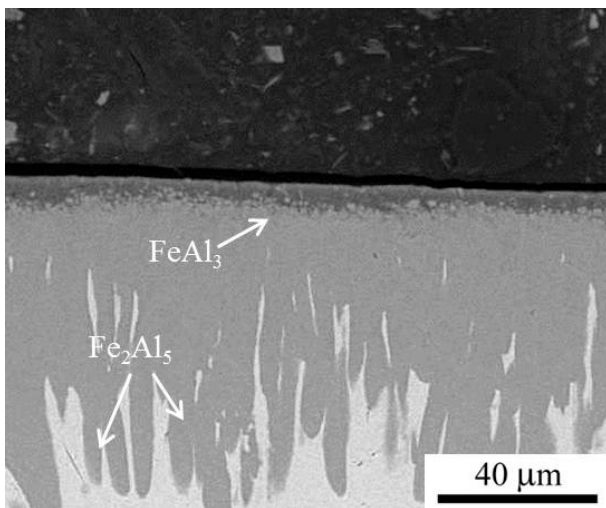

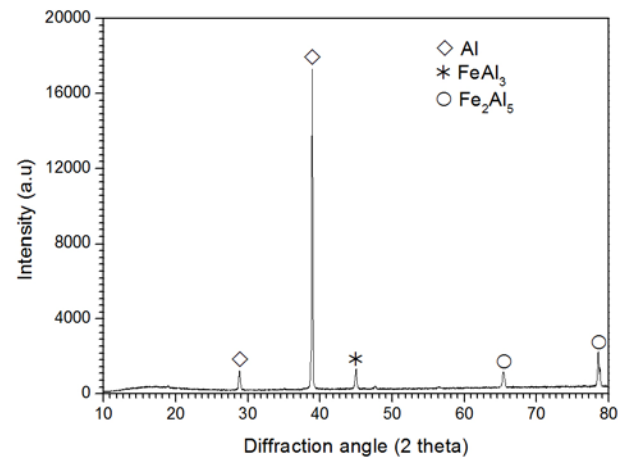**Figure 2** BEI of cross-sectional micrograph of the hot-dip aluminized AISI 1020 steel

Figure 3 XRD patterns of the aluminized steel

In order to understand the oxidation behavior and the phases formation of the aluminized steel, the oxidation test was carried out at 700 °C in static air for various durations of time. For 1-hour oxidation at 700 °C as shown in Figure 4, the aluminum topcoat could not be observed again in the coating layer. The aluminum topcoat disappeared and an aluminide layer formed owing to the outward diffusion of iron from the matrix and to the inward diffusion of aluminum. The aluminide layer being approximately 60 μm thick consists of a very thin Al_2O_3 layer on the surface, followed by a thicker layer of $Fe_2Al_5 + FeAl_2$ on the steel substrate side. However, the columnar morphology of Fe_2Al_5 (tongue-like morphology) can be still observed on the steel substrate.
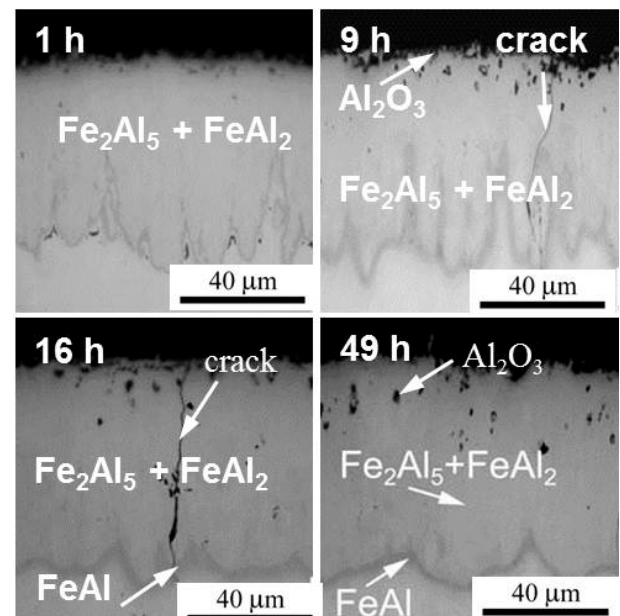

Figure 4 Optical microscopies of cross-sectional micrograps of the aluminized AISI 1020 steel oxidized at 700 °C for various duration of time

According to Figure 5, X-ray diffraction results confirm that there are three layers of intermetallic

layer formed e.i Fe_2Al_5, $FeAl_2$ and FeAl corresponding to the high intensity peaks after the aluminized steel was oxidized at 700 °C. But a low intensity peaks for Al_2O_3 was found for a sample oxidized for 1 h. For 9 h oxidation time, some voids formed in the aluminide layer as a result of phase transpormation, well known as Kirkendall effect (Chen & Wang 2006). Vacancies generated by interdiffusion between Al atoms and Fe atoms during phase transpormation in the aluminide layer condensed into voids. As shown in Figure 4, the black area in the aluminide layer was likely to be oxides formed from the specimen surface by high-temperature oxidation. In addition, for the oxidation time 9 h, the columnar structure of Fe_2Al_5 phase can be still observed in the aluminide layer, that indicates the rapid diffusion of Al atoms direction. Moreover, the thin FeAl layer is not clearly seen in the aluminide layer. The Fe_2Al_5 + $FeAl_2$ layer plays an important role as a reservoir of Al consumption to protect the steel by formation of protective Al_2O_3 layer. Consequently, many cavitations can be observed clearly, indicated as black area in outer part of aluminide layer as the oxidation time was increased to 16 h.

During oxidizing process, the outward diffusion of Al forms Al_2O_3 scale, and the other is Al inward diffusion toward the steel substrate. While the Fe inward diffusion into the Fe_2Al_5 + $FeAl_2$ layer leads to formation of FeAl layer. The phase consists of approximately 45 at.% Al. After oxidation time was increased to 49 h, the FeAl layer gradually thickened, as shown in Figure 4. The peaks corresponding to the FeAl phase shows the highest value in intensity (Figure 5). The aluminide layer thickness is relatively similar for all given oxidation time.
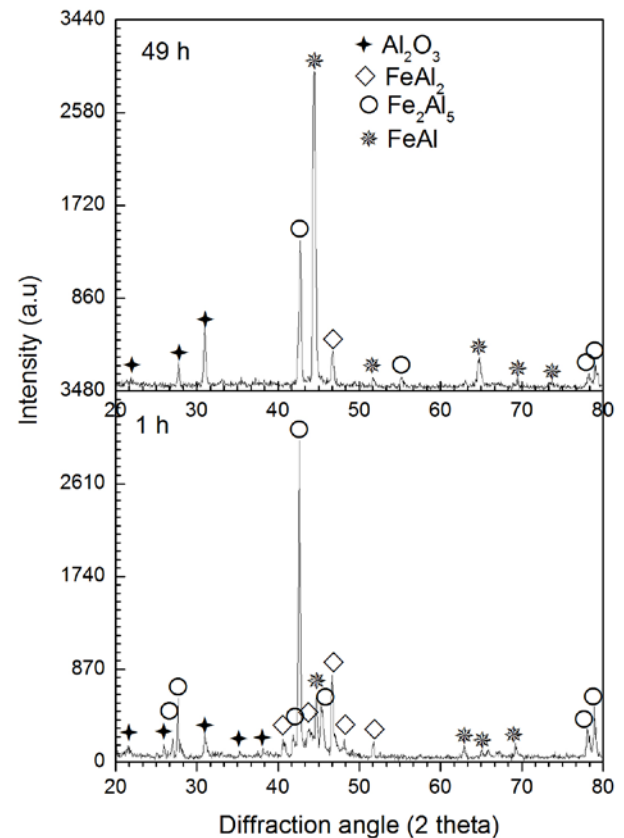

Figure 5 X-ray diffraction patterns analysis on the aluminized AISI 1020 steel oxidized at 700 °C

As shown in Figure 5, as the oxidation time was prolonged to 49 h, the intensity peak for the Fe_2Al_5 decreased, whereas the intensity peaks for the FeAl phase increased. One interesting about the formation of intermetallic layer during the oxidation process can also be observed that a cracks penetrate through the thickness of the aluminide layer when the oxidation time runs around 9 h (Figure 4). The thermal stresses induced into voids, lead to a crack generation in the aluminide layer (Chen & Wang 2006). After oxidation for 16 h, the columnar structure of the Fe_2Al_5 phase was reduced and then the second $FeAl_2$ layer was formed between the layer of Fe_2Al_5 layer and FeAl because the Al atoms diffused outwardly from the Fe_2Al_5 phase. While the inward diffusion of Fe atoms from the steel substrate into the Fe_2Al_5 + $FeAl_2$ layer generated the FeAl phase, as shown in Figure 4. For a longer oxidation time, the formation of FeAl phase seems that this phase formation is controlled by the inward diffusion of Fe atoms into the Fe_2Al_5 phase (Kobayashi & Yakou 2002).

As mentioned above, the low rate of oxidation of the aluminized steel is due to the formation of a protective Al_2O_3 scale formed on the aluminide layer. The Al_2O_3 scale on the aluminide layer during oxidizing process takes a place as diffusion barrier. This layer blocks the diffusion of oxygen into the aluminide layer, therefore the very thin alumina layer (Al_2O_3) is formed on the aluminide layer and this

layer is very protective to protect the steel from severe oxidation attack during service at high temperature. The availability of aluminum in the steel substrate is at least 5% in atomic composition to form a protective Al_2O_3 layer (Wang & Badaruddin 2010).
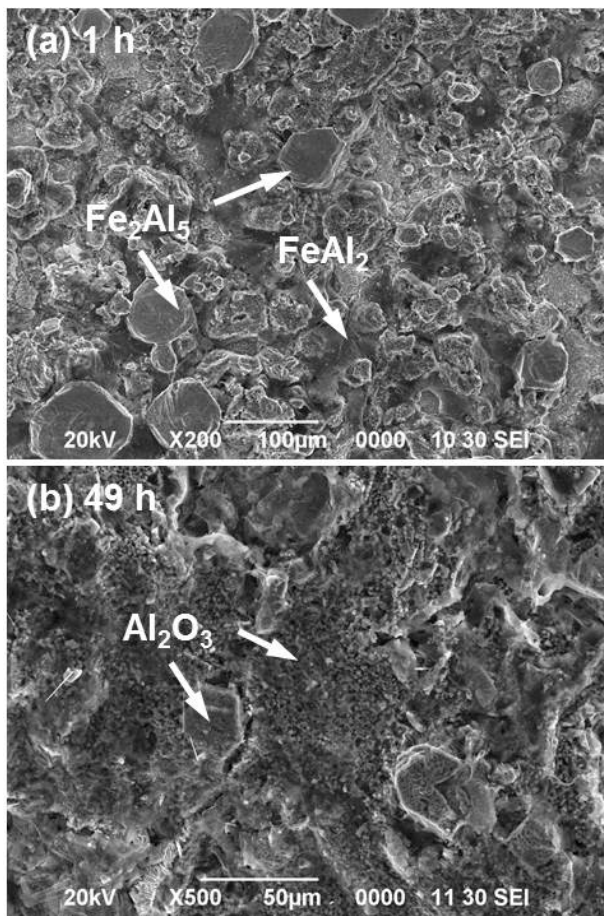

Figure 6 SEM of topography of the aluminized AISI 1020 steel subjected to isothermal oxidation at 700 °C

Meanwhile, through the top view investigation of scanning electron micrograph, it is clearly observed that the aluminum oxide formed on the coated specimen, as shown in Figure 6a. The formation of a protective layer was dominated by the phase intermetallic Fe_2Al_5. But for a longer oxidation time, forming a layer may be replaced by $FeAl_2$ phase (Figure 6b). The SEM micrograph in Figure 6 reveals the oxide morphology of the aluminized steel specimen after oxidation at 700 °C for 1–49 h; the surface morphology of the oxide scale reveals dense character, which consists of Al_2O_3. More voids and pores are observed in the aluminide layer.

Conclusion

The kinetics rate of the AISI 1020 steel can be decreased very significantly by the hot-dip aluminizing coating. The improvement of high temperature oxidation resistance of the aluminized steel is associated by the formation of protective Al_2O_3 scale. Formation of Fe−Al intermetallic layer during oxidation for a shorter oxidation time is dominated by interdiffusion between the outward diffusion of Al atom and the outward diffusion of Fe atom. Whereas, for a longer oxidation time the formation of FeAl phase is controlled by the diffusion of Fe atom into the Fe_2Al_5 phase. The formation of Al_2O_3 scale is supplied by Al atoms from both Fe_2Al_5 and $FeAl_2$ phase. The characteristic of Al_2O_3 scale are thin, dense and pores free formed on the hot-dip aluminized steel, giving a great contribution in protection of the AISI 1020 steel during oxidizing process at 700 °C for 49 h.

Acknowledgment

References

Qiao, L. & Yan, L.H. Stress corrosion cracking of AISI 321 stainless steel in acidic chloride solution. Material Science, Vol. 25, 47–51 (1998)

Kalivodova, J., Baxter, D., M. Schutze. & Rohr, V. Gaseous corrosion of alloys and novel coatings in simulated environments for coal, waste and biomass boilers. Materials and Corrosion, Vol. 56/12, 882–889 (2005)

Erlindo, C, Angcoy, Jr, Archibald, L.A, Romeo, P.A, Garry, F.C, Melvin, D.L, Christine H.S. & Ruperto R.V. Jr. Mechanisms of erosion-corrosion in Well 311D, South Sambaloran, Leyte Geothermal production field, Proceedings World Geothermal Congress, Bali, Indonesia (2010)

Ghosh, S.J. Failure analysis of a jacking oil pump, Failure Analysis and Prevention, Vol. 7, 23–27 (2007)

Cédric, N.H. Factors affecting costs geothermal power development, the Geothermal Energy Association for the U.S Department of Energy (2005)

Badaruddin M. Improvement of high temperature oxidation of low carbon steel exposed to ethanol combustion product at 700 °C by hot-dip aluminizing coating. Makara Seri Teknologi, 15/2,137–142 (2011)

Cheng, W.J. & Wang, C.J. Growth of intermetallic layer in the aluminide mild steel during hot-dipping. Surface & Coatings Technology, Vol. 204, 824–828

(2009)

Mc Kamey C.G. In: Stoloff N.S. & Sikka, V.K. Editors, Physical metallurgy and processing of intermetallic compounds. Chapman Hall, New York , 351 (1996)

Neumann, G. in: Mehrer, H. Edition. Diffusion in solid metals and alloys, numerical data and functional relationships in science and technology, Springer, Vol. 261, 152 (1999)

Kobayashi, S & Yakou, T. Control of intermetallic compound layers at interface between steel and aluminum by diffusion-treatment. Materials Science and Engineering A, Vol. 338, 44–53 (2002)

Chen, S.M. & Wang, C.J. The high-temperature oxidation behavior of hot-dipping Al–Si coating on low carbon steel. Surface & Coatings Technology, Vol. 200, 6601–6605 (2006)

Wang, C.J & Badaruddin, M. The dependence of high temperature resistance of aluminized steel exposed to water-vapour oxidation. Surface Coating & Technology, Vol. 205, 1200–1205 (2010)